# A GPC CONTROLLER ROBUSTIFICATION TOWARDS MEASUREMENT NOISE AND PARAMETER UNCERTAINTY CONSTRAINS

**P. Rodríguez*, D. Dumur*, E. Mendes†**

* Supélec F 91192 Gif sur Yvette cedex
phone: +33 (0)1 69 85 13 79/13 75 fax: +33 (0)1 69 85 13 89
e-mail: {pedro.rodriguez, didier.dumur}@supelec.fr

† Laboratoire de Génie Electrique de Paris (LGEP), CNRS, Supélec, Paris VI and XI. F 91192 Gif sur Yvette cedex
e-mail: mendes@lgep.supelec.fr

**Keywords:** GPC, robust control, Youla parametrisation, convex optimisation, linear programming.

## Abstract

This paper presents a methodology for enhancing the robustness of a GPC controlled system by convex optimisation of the Youla parameter. This methodology requires, as a first step, the design of an initial GPC controller; this controller is then robustified considering frequency and temporal constraints. By means of the Youla parametrisation, frequency and temporal constraints are formulated within a convex optimisation framework, then the optimal parameter is deduced solving this optimisation problem. The developed robustified GPC controller is finally applied on a benchmark including an induction motor, aiming at reducing the impact of measurement noise and inertia variation of the system, while respecting a temporal template for the disturbance rejection. Comparison with results obtained with a 'classical' PID controller is finally given.

## 1 Introduction

A classical technique to enhance qualities of GPC controllers is to make use of a model parameter as an additional degree of freedom. In this way, defining the prediction model in the classical CARIMA form, the $C$ polynomial modelling the noise influence may be used as a tuning parameter, since its identification is usually avoided. This approach is developed in [15]. It has been shown that the $C$ polynomial plays a crucial role in the robustness of the control law. More generally, this polynomial influences the robustness and disturbance rejection, unfortunately its choice remains complicated. Another way to introduce extra parameters is given by the $Q$-parametrisation [10]. It was first used in [9], to enhance robustness of the control. A robust optimisation problem is defined and an optimal $Q$ parameter is derived. This parameter is also considered in [1]. This $Q$-parametrisation can be referred to as a Youla type parametrisation, with additional implicit assumptions which restrict the result. The methods proposed in [9,15] provide high robustness bounds but penalise the disturbance rejection performance. The method proposed in [1] allows adjusting robustness/performance compromise but the Youla parameter is searched into a restricted set to make its choice simpler. Otherwise no disturbance rejection constraints are considered.

The purpose of this paper is to present a method enhancing the robustness of the controller towards model uncertainties, while respecting temporal constraints. As in [1] a two-step procedure is followed. An initial GPC controller is first designed with $C=1$, then the robustness of this controller is enhanced via the Youla parametrisation. This parametrisation allows formulating frequency and temporal constraints as convex optimisations. Afterwards, this optimisation problem is approximated by a linear programming, and the optimal $Q$ parameter belonging to the research set is derived.

Section 2 reminds the different steps required for the GPC controller design. Section 3 considers the Youla parametrisation of the system with the initial controller. In section 4, the frequency and temporal convex constraints are defined, and the related convex optimisation problem is transformed in a linear or quadratic programming under inequality constraints. Section 5 introduces the induction motor benchmark. Finally, section 6 provides the application of the control strategy to position control of an induction motor. These robustification results are shown and compared to those obtained with a feed-forward PID.

## 2 GPC design

This part briefly reminds the basic steps of the GPC controller design, more details may be found in [4,7]. In the GPC theory, the plant is modelled by the CARIMA form:

$$A(q^{-1})y(t) = B(q^{-1})u(t-1) + \frac{C(q^{-1})\xi(t)}{\Delta(q^{-1})} \qquad (1)$$

Where $u$ is the input, $y$ the output and $\xi$ is a zero mean white noise. The $C$ polynomial models the noise influence. The introduction of the difference operator $\Delta = 1 - q^{-1}$ in the disturbance model helps to find an integral action in the

controller and so eliminate static errors. $A$ and $B$ polynomials are obtained by a preliminary identification. The control signal is derived by minimisation of a quadratic cost function:

$$J = \sum_{j=N_1}^{N_2} \left[ w(t+j) - \hat{y}(t+j) \right]^2 + \lambda \sum_{j=1}^{N_u} \Delta u(t+j-1)^2 \qquad (2)$$

At this stage, it is assumed that the design has been performed with $C(q^{-1}) = 1$ and $N_1$, $N_2$, $N_u$, $\lambda$ adjusted to satisfy the required input/output behaviour. The resulting two-degrees of freedom *RST* controller will be denoted $R', S', T'$ in the following sections (Figure 1).

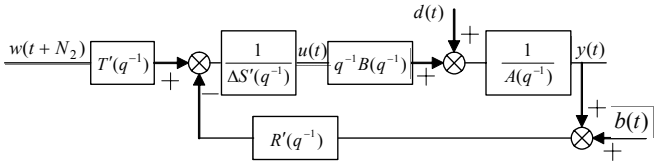


Figure 1: Two-degrees of freedom GPC controller.

## 3 Youla parametrisation

### 3.1 General consideration

Figure 2 considers a general feedback loop, with the classical notations, that will be used in our following developments.

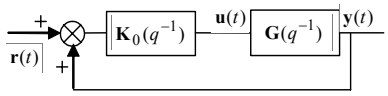


Figure 2: General feedback loop.

If $\mathbf{K}_0$ is a known stabilizing controller, any other stabilizing controller can be expressed as, see [10]:

$$\mathbf{K} = \mathbf{U}\,\mathbf{V}^{-1} = \widetilde{\mathbf{V}}^{-1}\widetilde{\mathbf{U}} \qquad (3)$$

Where:

$$\mathbf{U} = \mathbf{U}_0 + \mathbf{M}\,\mathbf{Q} \qquad \mathbf{V} = \mathbf{V}_0 + \mathbf{N}\,\mathbf{Q} \qquad (4)$$

$$\widetilde{\mathbf{U}} = \widetilde{\mathbf{U}}_0 + \mathbf{Q}\,\widetilde{\mathbf{M}} \qquad \widetilde{\mathbf{V}} = \widetilde{\mathbf{V}}_0 + \mathbf{Q}\,\widetilde{\mathbf{N}} \qquad (5)$$

and the fractional representations of $\mathbf{G}$ and $\mathbf{K}_0$ are chosen such that:

$$\mathbf{G} = \mathbf{N}\,\mathbf{M}^{-1} = \widetilde{\mathbf{M}}^{-1}\widetilde{\mathbf{N}} \qquad \mathbf{K}_0 = \mathbf{U}_0\,\mathbf{V}_0^{-1} = \widetilde{\mathbf{V}}_0^{-1}\,\widetilde{\mathbf{U}}_0 \qquad (6)$$

$$\begin{bmatrix} \widetilde{\mathbf{V}}_0 & -\widetilde{\mathbf{U}}_0 \\ -\widetilde{\mathbf{N}} & \widetilde{\mathbf{M}} \end{bmatrix} \begin{bmatrix} \mathbf{M} & \mathbf{U}_0 \\ \mathbf{N} & \mathbf{V}_0 \end{bmatrix} = \begin{bmatrix} \mathbf{I} & \mathbf{0} \\ \mathbf{0} & \mathbf{I} \end{bmatrix} \qquad (7)$$

### 3.2 Parametrisation of all stabilizing controllers for a two-degrees of freedom controller

In order to model the scheme of Figure 1 under the general feedback loop of Figure 2, the following system and initial controller are considered:

$$\mathbf{G}(q^{-1}) = \begin{pmatrix} 0 \\ \dfrac{q^{-1}B}{\Delta A} \end{pmatrix};\ \mathbf{K}_0(q^{-1}) = \begin{bmatrix} \dfrac{T'}{S'} & -\dfrac{R'}{S'} \end{bmatrix};\ \mathbf{r} = \begin{pmatrix} w \\ b \end{pmatrix};\ \mathbf{y} = \begin{pmatrix} 0 \\ y \end{pmatrix} \qquad (8)$$

The integral action is included in the system, which permits to parametrise all controllers that stabilise the system and keep the integral action. With this structure the fractional representations of the system and the initial controller of Equation (9) have been chosen, with $A_o A_c = \Delta A S' + q^{-1} B R'$ the characteristic polynomial of the closed loop obtained with $\mathbf{K}_0$. This polynomial is split, like in pole placement see [2], into a control polynomial $A_c$ and an observer polynomial $A_o$, both stable because $\mathbf{K}_0$ is a stabilizing controller. Each transfer of the fractional representation (9) is therefore stable.

$$\mathbf{N} = \begin{pmatrix} 0 \\ \dfrac{q^{-1}B}{A_c} \end{pmatrix} \quad \widetilde{\mathbf{N}} = \begin{pmatrix} 0 \\ -\dfrac{q^{-1}B}{A_o} \end{pmatrix} \quad \widetilde{\mathbf{M}} = \begin{pmatrix} -1 & 0 \\ 0 & -\dfrac{\Delta A}{A_o} \end{pmatrix} \quad \mathbf{M} = \frac{\Delta A}{A_c}$$

$$\mathbf{U}_0 = \begin{pmatrix} -\dfrac{\Delta A T'}{A_o A_c} & \dfrac{R'}{A_c} \end{pmatrix} \qquad \widetilde{\mathbf{U}}_0 = \begin{pmatrix} \dfrac{T'}{A_o} & -\dfrac{R'}{A_o} \end{pmatrix} \qquad (9)$$

$$\mathbf{V}_0 = \begin{pmatrix} -1 & 0 \\ -\dfrac{q^{-1}BT'}{A_o A_c} & -\dfrac{S'}{A_c} \end{pmatrix} \quad \widetilde{\mathbf{V}}_0 = \frac{S'}{A_o}$$

This fractional representation satisfies Equations (6,7). Applying Equation (4) or (5), all stabilizing controllers can be deduced, considering $\mathbf{Q} = [Q_2 \quad Q_1]$, under the form:

$$\mathbf{K}(q^{-1}) = \begin{bmatrix} \dfrac{T' - A_o Q_2}{S' - q^{-1} B Q_1} & -\dfrac{R' + \Delta A Q_1}{S' - q^{-1} B Q_1} \end{bmatrix} \qquad (10)$$

Where $Q_1$ and $Q_2$ are free stable transfer functions. The $Q_2$ parameter modifies the input/output transfer function, whereas the $Q_1$ parameter modifies the closed loop characteristic keeping the input/output transfer unchanged, see [14,11]. The *Q* parametrisation presented by Kouvaritakis *et al.* in [9] is obtained from Equation (10) with $Q_2 = 0$.

## 4 Frequency and temporal constraints

### 4.1 Frequency constraints – Stability robustness

Let consider an unstructured uncertainty, as shown Figure 3.

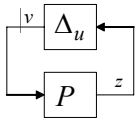


Figure 3: Unstructured uncertainty.

Where *P* represents the system connected to the uncertainty block. The formulation of this system depends in fact on the uncertainty representation, which can be additive, multiplicative, direct or inverse. Table 1 summarises the transfers connected to the uncertainty under the different representations, see [6], assuming the system and controller structured as in Figure 1. Considering the small gain theorem [10,11], the robustification towards unstructured uncertainties is maximised formulating an $H_\infty$ norm minimisation:

$$\min_{Q_1 \in \Re H_\infty} \left\| P(q^{-1}) W(q^{-1}) \right\|_\infty \qquad (11)$$

*W* is a weighting transfer function. The Youla parametrisation allows linear dependency between the *P* transfers and the

Youla parameter as shown in Table 1, so the specifications defined by Equation (11) are convex in $Q_1$, see [3,5].

| $\Delta_u$ | $P$ |
|---|---|
| additive direct | $-\frac{R'A}{A_o A_c}-\frac{A^2\Delta}{A_o A_c}Q_1$ |
| additive inverse | $\frac{q^{-1}B\Delta S'}{A_o A_c}-\frac{q^{-2}B^2\Delta}{A_o A_c}Q_1$ |
| multiplicative direct | $-\frac{q^{-1}BR'}{A_o A_c}-\frac{q^{-1}B\Delta A}{A_o A_c}Q_1$ |
| multiplicative inverse | $\frac{S'\Delta A}{A_o A_c}-\frac{\Delta A q^{-1}B}{A_o A_c}Q_1$ |

Table 1: *P* function connected to the uncertainty blocks.

### 4.2 Temporal constraints

In our further developments, we will assume that the initial controller has been adjusted to provide the desired behaviour of the *y*/*w* transfer, in this case the $Q_2$ parameter must be zero to maintain this transfer unchanged. Considering the influence of the disturbances $d(t)$ and $b(t)$ on the signals $u(t)$ and $y(t)$, the following transfer functions, with $d(t)$ and $b(t)$ as inputs, $u(t)$ and $y(t)$ as outputs, must be taken into account as basis for the temporal constraints problem:

$$\begin{pmatrix}u(t)\\y(t)\end{pmatrix}=\begin{pmatrix}H_{ud} & H_{ub}\\H_{yd} & H_{yb}\end{pmatrix}\begin{pmatrix}d(t)\\b(t)\end{pmatrix}$$
$$=\begin{pmatrix}-\frac{R'}{A_o A_c}-\frac{\Delta A}{A_o A_c}Q_1 & -\frac{R'A}{A_o A_c}-\frac{A^2\Delta}{A_o A_c}Q_1\\ \frac{\Delta S'}{A_o A_c}-\frac{q^{-1}B\Delta}{A_o A_c}Q_1 & -\frac{q^{-1}BR'}{A_o A_c}-\frac{q^{-1}B\Delta A}{A_o A_c}Q_1\end{pmatrix}\begin{pmatrix}d(t)\\b(t)\end{pmatrix} \quad (12)$$

These transfers are linearly parametrised by the Youla parameter. This allows convex specifications for the temporal template constraints, see [3,5]. Let denote $s_{ij}(t)$ the response of $H_{ij}$ to a specific input. The temporal specification consists of a template inside which $s_{ij}(t)$ must remain constrained. The set of all $Q_1$ parameters that satisfy this constraint is:

$$\begin{aligned}C_{env}&=\left\{Q_1 / \forall t\geq 0; s_{\min}(t)\leq s_{ij}(t)\leq s_{\max}(t)\right\}\\&=\left\{Q_1 / \Phi_{env}(Q_1)\leq 0\right\}\end{aligned} \quad (13)$$

With:

$$\Phi_{env}(Q_1)=\max\left(\max_{t\geq 0}\left(s_{ij}(t)-s_{\max}(t), s_{\min}(t)-s_{ij}(t)\right)\right) \quad (14)$$

These temporal specifications can be used to model the dynamic of the controller, since normally the disturbances entering the system at *d* and *b* points are unknown.

### 4.3 Resolution by linear programming

The problem aims at finding $Q_1 \in \Re H_\infty$ that minimises a $H_\infty$ norm under the constraints imposed by temporal specification. This convex optimisation problem leads to a $Q_1$ parameter which varies in an infinite-dimensional space. There is nowadays no solution to this optimisation problem. One possibility providing a sub-optimal solution is to consider a finite-dimensional sub-space generated by an orthonormal base of stable transfer functions:

$$Q_1=\sum_{i=0}^{n_q}\alpha_i Q_{1i} \quad (15)$$

With such a $Q_1$ parameter base, the $H_\infty$ norm minimisation and the temporal constraints can be approximated by linear inequalities, and the optimisation problem can be solved by a minimisation under inequality constraints [13].

## 5 Experimental setup and position benchmark

### 5.1 Experimental set-up

The experimental set-up of the 'Laboratoire de Génie Electrique de Paris' (LGEP) in Gif sur Yvette, France, includes an induction machine control. The pulse width modulation (PWM) control of the inverter is implemented in a PC with the real-time RT-Linux operating system [8].

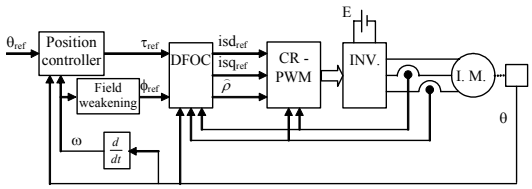


Figure 4: Structure of the direct field-oriented control (DFOC) with a position loop controller.

The motor characteristics are: Power 1.1 Kw , nominal torque $\tau_{nom}=7$ Nm . The position sensor has 14400 points per rotation. Figure 4 shows the position control architecture. The internal control is a direct field-oriented control (DFOC), with a sample rate of 76.6µs. In the external loop the field weakening assures that the flux reference decreases when the nominal speed of the motor has been exceeded. The position controller provides position tracking performance.

### 5.2 Benchmark

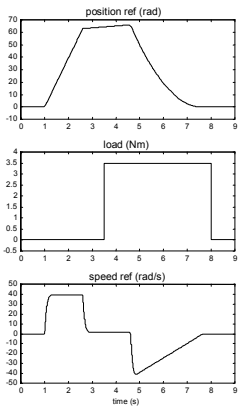


Figure 5: Benchmark position trajectories - "slow" cycle.

To compare different controllers, a position benchmark with two cycles is used: one 'slow' cycle, where the speed reference is close to the nominal speed, and one 'fast' cycle, where the speed reference is higher than the nominal speed. Due to restricted place, only results with the 'slow' cycle are reported. In the 'slow' cycle, see Figure 5, the rotor flux is constant. This cycle enables to test the position loop behaviour at very slow and zero speeds with load variation, at nominal speed and during parabolic position tracking.

# 6 Experiments

## 6.1 Prediction model for GPC design

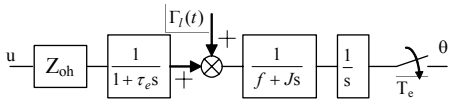


Figure 6: Model for the GPC design.

Figure 6 shows the model used for the GPC design. The $\tau_e$ constant represents the current loop, the DFOC and the inverter dynamics. This time constant is neglected in further developments compared to the mechanical time constant. The motor and the load are represented by $J$, $f$ and $\Gamma_l$. The system is sampled at $T_e = 1.0724\,\text{ms}$. The discrete time model obtained for $J = 0.007\,\text{Kg m}^2$ and $f = 0.01\,\text{Nm rad}^{-1}\,\text{s}$ is:

$$\frac{\theta(q^{-1})}{u(q^{-1})} = \frac{10^{-4}(0.821q^{-1} + 0.8206q^{-2})}{(1-q^{-1})(1-0.998q^{-1})} \qquad (16)$$

## 6.2 First step: Classical GPC design with $C = 1$

An initial GPC controller has been designed with $C = 1$ and the following tuning parameters, selected according to the rules given in [7], $N_1 = 1, N_2 = 16, N_u = 1, \lambda = 0.0001$.

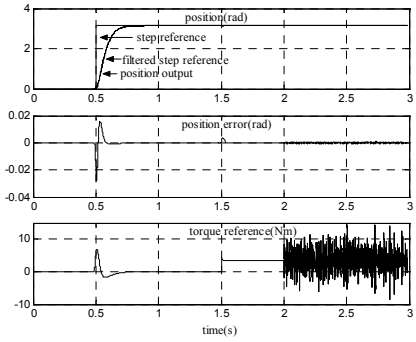


Figure 7: Responses with the initial GPC controller.

The impact of this controller has been tested first in simulation. The position, position error and torque signals responses to a filtered step set point and to a step disturbance signal are given in Figure 7. The disturbance corresponds to a step load increase of 3.5 Nm added at $t = 1.5\,\text{s}$. For this simulation, a zero mean pseudo random measurement noise of $(2\cdot10^{-4})^2$ variance is added to the output at $t = 2\,\text{s}$. This noise power is approximately the noise power of the benchmark position sensor. The influence of this noise on the position error and on the control signal clearly appears.

## 6.3 Second step: Robustification

This initial controller can not be experimentally implemented because of the effect of the measurement noise in the command. The first idea is thus to robustify the controller in order to decrease this effect. To do so, the measurement noise can be considered as an additive uncertainty and the corresponding $P$ function of table 1 has to be minimised. This is the approach used in [9,15]. However, this robustification decreases the dynamic of the closed loop, and consequently the dynamic of the disturbance rejection. In order to impose disturbance rejection constraints and find a Youla parameter that guaranties the disturbance rejection dynamic, a temporal template can be used which constraints the disturbance rejection response. This is the approach developed in [13]. In this paper, the uncertainties in the inertia of the system are also considered. This kind of uncertainty can be modelled by a multiplicative direct unstructured uncertainty. Table 1 shows the function that must be minimised in order to robustify towards this kind of uncertainty. This transfer corresponds to the complementary sensitivity function of the system. In order to find a Youla parameter that robustifies the initial GPC towards an uncertainty on the inertia, that also reduces the effect of measurement noise on the control, and that assures a sufficiently fast dynamic for the disturbance rejection, the following optimisation problem is considered:

$$\min_{\substack{Q_1 \in \Re H_\infty \\ \Phi_{env1}(Q_1)<0 \\ \Phi_{env2}(Q_1)<0}} \left\| \left( -\frac{q^{-1}BR'}{A_o A_c} - \frac{q^{-1}B\Delta A}{A_o A_c} Q_1 \right) W(q^{-1}) \right\|_\infty \qquad (17)$$

In this optimisation problem, the minimisation of the complementary sensitivity function, that is the $P$ function of the direct multiplicative model uncertainty case, is considered, satisfying two temporal templates. $\Phi_{env1}(Q_1)$ corresponds to a temporal template for the disturbance rejection, this template is shown in Figure 8. $\Phi_{env2}(Q_1)$ corresponds to a temporal template for the measurement noise/control transfer $u(t)/b(t)$ (a frequency specification could have also been used). With a pseudo random noise of zero mean and $(2\cdot10^{-4})^2$ variance, this specification fixes a limit in the measurement noise effect on the control, restricting variations of $u(t)$ due to noise within a $\pm0.1$ range.

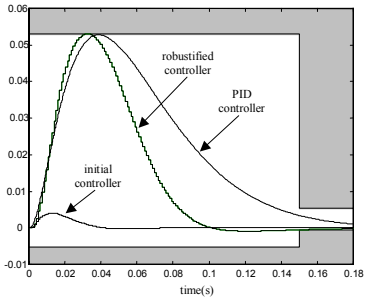


Figure 8: Temporal template for disturbance rejection.

A $Q_1$ parameter search has been performed via quadratic minimization algorithm under inequality constraints. The following parameter has been deduced:

$$Q = \frac{-6979.05 + 30860.3q^{-1} - 56836.79q^{-2} + 55985.24q^{-3} - 31194.51q^{-4} + 9321.26q^{-5} - 1157.22q^{-6}}{(1-0.7q^{-1})(1-0.8q^{-1})(1-0.93q^{-1})(1-0.94q^{-1})(1-0.95q^{-1})(1-1.1884q^{-1}+0.41282q^{-2})} \quad (18)$$

Using the orthonormal base described in [12]:

$$Q_{1i}(q^{-1}) = \frac{\sqrt{1-|\varepsilon_i|^2}}{1-\varepsilon_i q^{-1}} \prod_{k=0}^{i-1} \frac{q^{-1}-\bar{\varepsilon}_k}{1-\varepsilon_k q^{-1}} \quad (19)$$

The optimisation has been solved with the following parameters for the base of the Youla parameter: $\varepsilon_0 = 0.7$, $\varepsilon_1 = 0.8$, $\varepsilon_2 = 0.93$, $\varepsilon_3 = 0.94$, $\varepsilon_4 = 0.95$, $\varepsilon_5, \varepsilon_6$ are defined by a pair of complex conjugated poles corresponding to the continuous ones of natural pulsation $\omega = 550$ rad/s and damping factor $\zeta = 0.75$. The considered weighting function is:

$$W = \frac{1-0.7q^{-1}}{0.3} \quad (20)$$

Figure 9 shows the measurement noise/command transfer for the initial and robustified controllers, and for a PID with feed-forward controller that will be used in the following to compare the experimental results. The robustified controller has a more important high frequency measurement noise rejection than the initial controller. Figure 10 shows the complementary sensitivity function of the closed loop with the designed controller. The parameter found is the one that has the minimum $H_\infty$ norm for this transfer satisfying at the same time the temporal constraints. Figure 8 shows that the disturbance rejection satisfies the temporal template.

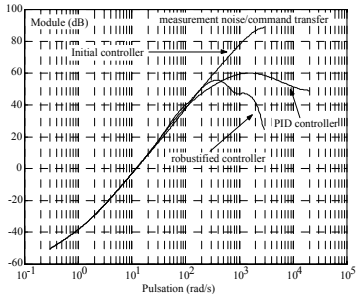


Figure 9: Measurement noise/command function.

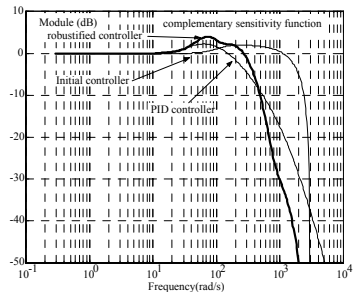


Figure 10: Complementary sensitivity function.

### 6.4 Experimental results

The robustified GPC controller previously developed has been implemented on the benchmark, providing the results of Figure 11. The results for the robustified GPC controller are compared to the ones obtained with a PID running at 176.6µs, with a feed-forward and a filter in the derivative action (Figure 12). These figures show the position error and the control signal. For the GPC controller the obtained behaviour is faster and the position error is smaller with nearly the same noise in the control signal. The robustified GPC efficiently rejects the noise on the control signal. In fact, the PID controller provides the same effect with an adequate choice of the derivative filter, but with a slower tracking dynamic.

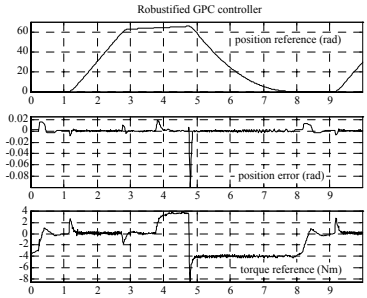


Figure 11: Position response and control signal for the robustified GPC controller– Nominal system.

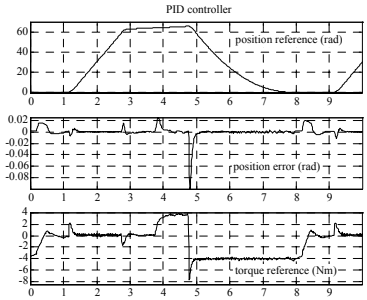


Figure 12: Position response and control signal for the PID controller– Nominal system.

Figures 13 and 14 show the results obtained under the same conditions for both robustified GPC and feed-forward PID controllers, but with $J = 0.01\text{kg m}^2$. With this inertia the position tracking is faster for the PID controller but the disturbance rejection is faster for the robustified GPC controller. The control signal has no oscillation for the GPC controller and has oscillations for the PID controller. This oscillation in the command signal is induced by a neglected dynamic that appears in the system with the additional inertia. This neglected dynamic affects the PID but does not affect the GPC controller. In Figure 9 the $P$ function for additive uncertainties, that is, the measurement noise/command transfer, is smaller for the robustified GPC controller than for the PID. Consequently, the GPC controller can accept higher additive uncertainties without loss of stability.

The experimental results show that the presented method allows to robustify an initial controller according to several

constraints. In this case the initial controller has been robustified to minimise the influence of neglected dynamics and measurement noise. It also guaranties some robustness performance when the inertia of the system varies and guaranties a desired dynamic for the disturbance rejection.

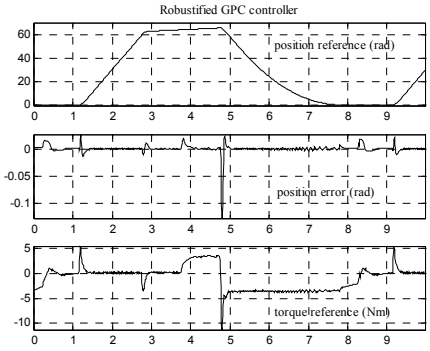


Figure 13: Position response and control signal for the robustified GPC controller – Modified inertia.

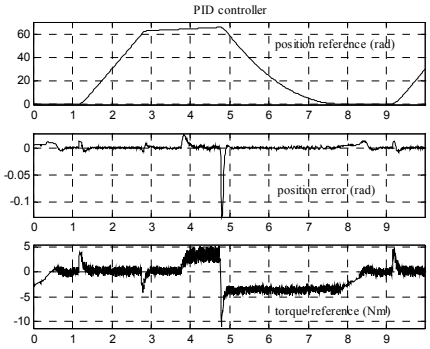


Figure 14: Position response and control signal for the PID controller– Modified inertia.

## 7 Conclusions

This paper presents a design method based on the Youla parametrisation to enhance the robustness of a GPC controller while respecting temporal constraints. Both frequency and temporal constraints are first formulated as a convex optimisation problem thanks to the parametrisation of all stabilizing controllers operated by the Youla parameter. However, as this parameter belongs to an infinite-dimensional space, the optimal solution can not yet be found. A sub-optimal solution belonging to a sub-space generated by an orthonormal base is deduced.

This method has been applied to a GPC controlled positioning system. The realised optimisation takes into account the measurement noise effect on the command signal, the disturbance rejection and an uncertainty on the inertia of the system. The resulting controller has been implemented on a benchmark including an induction motor. The experimental results have been compared to those obtained with a PID. It has been shown that better results can be noticed with the method presented in this paper, and that temporal templates permit simple visual adjustment of the robustness and dynamics bounds. The influence of the approximations during frequency optimisation and the choice of the orthonormal base for the subspace generation are open points to future works.

## References


[1] P. Ansay, M. Gevers and V. Wertz, “Enhancing the robustness of GPC via a simple choice of the Youla parameter”, European Journal of Control, **4**, pp. 64-70, 1998.

[2] K.J. Åström and B. Wittenmark, “Computer controlled systems. Theory and design (Third Edition)”, Prentice Hall, Englewood Cliffs, N.J. 1997.

[3] S. Boyd and C. Barrat, “Linear Controller Design. Limits of performance”, Prentice Hall, 1991.

[4] D.W. Clarke and C. Mohtadi, “Properties of generalized predictive control”, Automatica, **25(6)**, pp. 859-875, 1989.

[5] B. Clément, S. Hbaïeb, G. Duc et S. Font, “Paramétrisation de Youla : application à la commande robuste par optimisation convexe”, APII Journal Européen des Systèmes Automatisés, **35(1-2)**, pp. 33-48, 2001.

[6] J.M. Dion and D. Popescu, “Commande Optimale”, Diderot Editeur, Arts et Sciences, 1996.

[7] D. Dumur and P. Boucher, “A Review Introduction to Linear GPC and Applications”, Journal A, **39(4)**, pp. 21-35, 1998.

[8] C. Gi-Won, G. Espinosa, E. Mendes and R. Ortega, “Tuning rules for the PI gains of field-oriented controllers of induction motors”, IEEE Transactions on industrial electronics, **47(3)**, pp. 592-602, 2000.

[9] B. Kouvaritakis, J.A. Rossiter and A.O.T. Chang, “Stable generalised predictive control: an algorithm with guaranteed stability”, IEE Proceedings-D, **139(4)**, pp. 349-362, 1992.

[10] J.M. Maciejowski, “Multivariable feedback design”, Addison-Wesley publishing company, Wokingham, England, 1989.

[11] M. Morari and E. Zafiriou, “Robust Process Control”, Prentice Hall, Englewood Cliffs, N.J. 1989.

[12] B. Ninness and F. Gustafsson, “A Unifying Construction of Orthonormal Bases for System Identification”, IEEE Transactions on automatic control, **42(4)**, pp. 515-521, 1997.

[13] P. Rodriguez and D. Dumur, “Robustification of GPC controlled system by convex optimisation of the Youla parameter”, Proceedings of the IEEE Conference on Control Applications, Glasgow, 2002.

[14] M. Vidyasagar, “Control System Synthesis – A Factorization Approach”, MIT Press, Cambridge, MA 1985.

[15] T.W. Yoon and D.W. Clarke, “Observer design in receding-horizon predictive control”, International Journal of Control, **61(1)**, pp. 171-191, 1995.